Comparative core analysis from a Wolfcamp formation well; a case study

Joel Walls*, Anyela Morcote*, Tiffany Hintzman*, Michael Everts**
*Ingrain Inc., Houston, TX; **Halliburton, Houston, TX

This paper was prepared for presentation at the International Symposium of the Society of Core Analysts held in Snow Mass, Colorado, USA, 21-26 August 2016

ABSTRACT

The Permian Basin Wolfcamp shale formation is a prolific producer of oil and gas from horizontal wells. The formation is over 1000 feet thick in most areas and has multiple prospective completion targets. The Wolfcamp formation is also highly variable in mineralogy, total organic content (TOC), porosity and other key reservoir properties. For this project, a full diameter core of 246 feet length was obtained, and a multi-faceted core analysis program was conducted. The program included spectral gamma logging, dual-energy CT imaging, plug sample selection, geochemistry, traditional shale core analysis, and digital rock analysis. Digital rock data from plug sample was upscaled to the whole core scans and continuous vertical curves were computed for mineralogy, brittleness index, TOC, porosity, and permeability.

Plug samples were taken from 34 depth locations selected to be representative of the key lithologies as indicated by the bulk density (RHOB) and photo-electric factor (PEF) computed from dual-energy CT imaging. Preserved plug samples were sent to three different labs for physical lab testing, geochemistry, and digital rock analysis. One objective of this project was to obtain key reservoir and completion quality data to aid in selecting an optimum horizontal landing zone and to quantify hydrocarbon in place. Another goal was to enable comparisons between physical lab and digital rock experiments. Using ion-milled SEM images and 3D FIB-SEM data, TOC, intergranular porosity, and porosity associated with organic matter (PAOM) were determined. Of particular interest was to understand the importance of PAOM and to explore the similarities and differences between SEM derived porosity and helium porosity from traditional physical lab test.

INTRODUCTION

The subject well for this project was drilled in the Delaware Basin in west Texas, USA, and was sampled in the upper Wolfcamp formation. In order to gain a more thorough understanding of reservoir and completion-related rock properties, an extensive suite of core and well log data was obtained. Approximately 246 feet (75 meters) of full diameter core was recovered and it was immediately cut into 3 foot long sections while still inside the aluminum inner core barrel liner. These individual tubes were sealed with rubber end caps to reduce sample loss and drying, then shipped directly from the field to the digital rock lab.

METHODS

For this project, the entire core was CT and spectral gamma ray (SGR) scanned while still sealed in the aluminum core barrel liners. From this imaging, a continuous high-resolution (about 1000 points per linear foot) log was computed of RHOB and PEF using a process described by Vinegar, 1986 and Coenen and Maas, 1994. By combining SGR with RHOB and PEF, estimations of rock mineral volumes, clays, silicates, and carbonates were computed, as well as TOC. X-ray fluorescence (XRF) data was acquired at discrete points along the core for mineral volume calibration purposes.

In order to select plugs and ensure adequate characterization of the rocks with greatest reservoir potential, the data was divided into classes as described by Walls and Sinclair, 2011. From each of the 34 selected plugs, a half inch end trim was removed and used for digital rock analysis. The remaining portion of the plug and the second plug taken at the same depth was used for quantitative XRD, LECO, TOC and other tests.

To aid with sub-sample selection for SEM imaging, Archimedes bulk density was measured from the end trim, bulk TOC and mineralogy was measured from homogenized material using Fourier Transform Infrared Spectroscopy (FTIR) and a three component mineralogy classification was computed based on XRF measurements. From each sub-sample, a 1 millimeter by 0.5 millimeter argon ion polished area was SEM imaged using both secondary electron (SE2) and back-scatter electron (ESB1) detectors at 10 nanometers per pixel. The sets of high resolution images were combined and segmented for porosity, organic matter, higher density minerals, and matrix grains. The porosity was further analyzed and separated into PAOM, intergranular and intragranular porosity.

For this project, 8 of the 34 plug samples had a 3D image data set acquired with a FIB-SEM imaging system by alternately removing 15 nanometers of material with the Ga+ ion beam and then acquiring SE2 and ESB1 images simultaneously at a resolution of 15 nanometers per pixel. Each 3D volume was segmented into grain, porosity, and organic matter. From the effective pore volume, connected and isolated porosities were computed as well as PAOM. Horizontal and vertical absolute permeability was computed with the use of Lattice-Boltzmann methods on the connected pore volume.

RESULTS

Mineral composition was measured with XRF and XRD from 34 samples. From each analysis, a 3 component mineralogy group comprising of clays, silicates, and carbonates was normalized and plotted onto a ternary diagram. The results from both techniques are in good agreement with each other. The datasets show similar mineralogy distribution with silica to clay ratio of about 70/30 and the carbonate content ranging from 0-90% by weight. Each data point in Figure 1 represents the mineralogy for one sample. The data points are also colored by rock classes characterized by the high resolution RHOB and PEF obtained from the dual energy CT scan of the core.

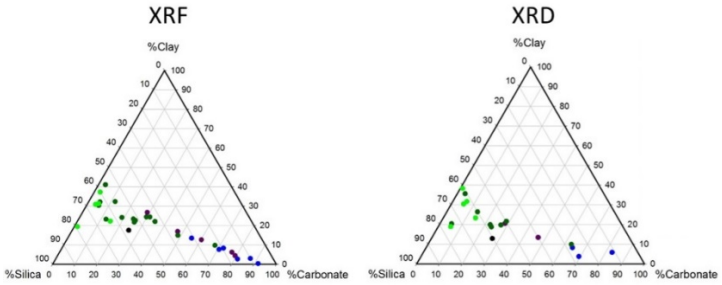

Figure 1: Comparison of mineralogy results from XRF (left) and XRD (right).

From the 34 plug samples, PHIE, organic matter, and PAOM were segmented and measured from 10 SEM image data sets per sample. Each of the 10 pairs of images (secondary and backscatter electron) span an area of approximately 20 X 30 microns. The results were averaged per sample and are used for observations and comparisons. The 34 samples show a wide range of porosity, organic matter and mineralogy. Each data point in Figure 2 represents the average for a sample. The data points are also colored by rock classes. The more siliceous samples (green and black data points) range in porosity from 1 to 6% by volume and range in PAOM from 0.5 to 2% by volume. The more calcareous samples (blue and purple data points) range in porosity from 0.5 to 5% and range in PAOM from 0 to about 1% by volume. Most samples have a combination of mineral bounded (intergranular plus intragranular) porosity and porosity associated with organic matter. In Figures 3 the segmented PAOM from the image to the left is shown in blue and the segmented intergranular porosity is in red.

LECO TOC from geochemical lab analysis was measured and compared to organic matter from SEM for 13 samples with closely matching depths. The results in Figure 4 show that the SEM total organic matter and LECO TOC form a linear trend that has a non-zero intercept. The higher LECO TOC values in the cluster of four low TOC samples may have been caused by incomplete calcite dissolution as these were all high calcite samples. Also we do not know the kerogen density exactly so it isn't possible to convert weight % to volume % exactly, but a factor of 2 is a common assumption. The dashed line in Figure 4 shows the line of equality (slope = 1) between SEM and LECO with the factor of 2 assumption. For 13 samples, the average equivalent Vro is 1.18 and the average Tmax is 463 (late oil to early gas window).

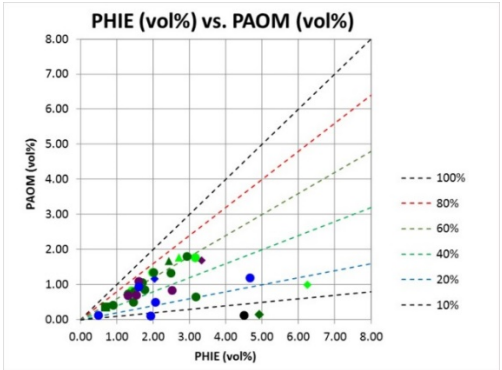

Figure 2: Crossplot of PHIE and PAOM from SEM. Data points colored by CT class.

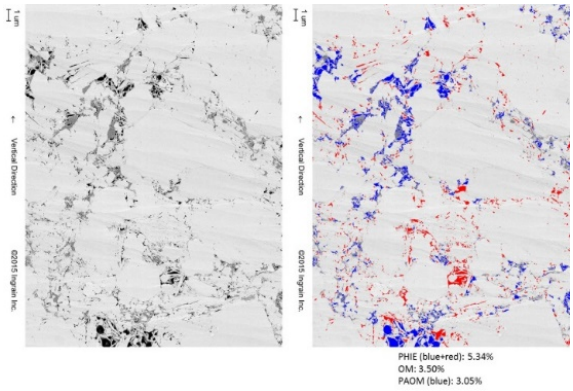

Figure 3: Left is an original 10 nm/pixel SE2 image, and right is a segmented image with intergranular porosity in red and organic porosity in blue.

The clay bound water volume cannot be resolved from SEM images and gets counted as part of the clay mineral volume during image analysis. Therefore the SEM porosity can be considered as porosity available for free water or hydrocarbons, which is a common definition of effective porosity (PHIE). Clay in these samples is about 19% smectite and 81% illite as determined by XRD. The weighted average clay bound water porosity is equal to about 0.18 times total clay volume using Chitale's published clay porosity for different clay species. This clay bound water (CBW) porosity was added to effective porosity from SEM imaging to get an approximate total porosity.

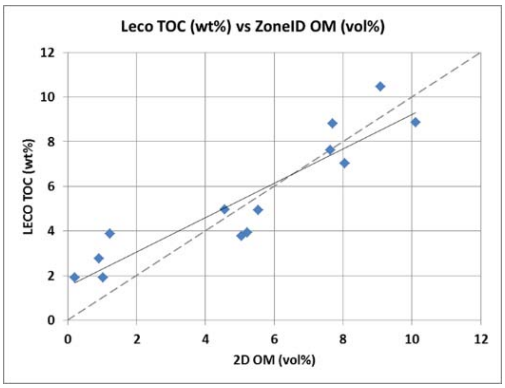

Figure 4: Comparison of organic matter from 2D SEM to LECO TOC for subset of samples with exactly matching depths. Low TOC samples had high calcite content which may have increased LECO TOC if there was incomplete calcite dissolution.

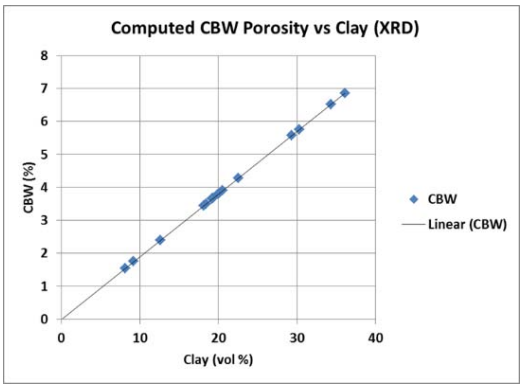

Figure 5: Computed clay bound water (CBW) porosity using results from Chitale, 2010 combined with clay analysis from XRD.

From eight 3D FIB-SEM volumes, the properties computed were connected porosity, isolated porosity, PAOM, organic matter, and absolute permeability in both the vertical and horizontal directions. The porosity from these 3D volumes ranged from 4 to 11% by volume. The horizontal absolute permeability ranged from about 40 to 1900 nD. The porosity versus horizontal permeability trend was determined and compared to porosity and permeability from GRI crushed sample analysis. The porosity ranges for both types of data are similar and so are the porosity-permeability trends (Figure 6). We could not cross plot porosity vs porosity or permeability vs permeability for the two methods because none of the depths of the FIB-SEM and GRI samples matched.

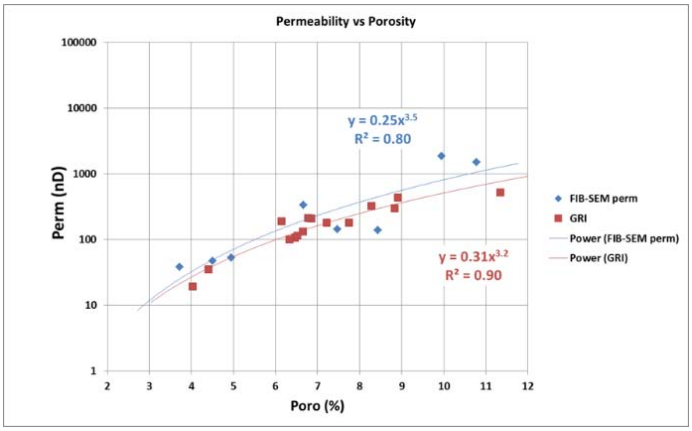

Figure 6: FIB-SEM computed porosity and permeability trend compared to GRI data. (not matching depths)

Petrophysical Integration and Upscaling:

The SEM and FIB-SEM analysis and results from selected plugs were incorporated into the petrophysical analysis as calibration points. Thus, we were able to estimate total porosity (PHIT), effective porosity (PHIE) and PAOM as continuous logs along the cored interval. Since matrix permeability was computed at various depths from a 3D FIB-SEM volume using a Lattice Boltzmann method (Tolke, et al., 2010), a matrix permeability log was obtained from the correlation between FIB-SEM porosity and computed permeability. Using a combination of X-ray CT data, SGR, SEM, and FIB-SEM analysis, key shale reservoir rock properties were computed along the entire cored interval (Figure 7). This analysis contributed to a better understanding of this well at an early stage of the study process.

These rocks have a wide variability in mineralogy, porosity, and TOC over short vertical distances. The CT scan data was able to detect and resolve the thin layers. Brittleness index (BI), was based on a relationship between Young's modulus and Poisson's ratio, similar to that of Rickman, et al., 2008. Estimation of BI shows that the most calcareous rocks are generally more brittle than the more clay rich rocks. However, the tight, high calcite layers also have high rock strength which can act as a barrier to vertical fracture growth depending on the layer thickness and spacing.

OBSERVATIONS AND CONCLUSIONS

Some key findings from this project are;

- LECO TOC from geochemical lab analysis matches organic matter from SEM with a correlation coefficient R^2 of 0.84.
- SEM image derived porosity is analogous to effective porosity (hydrocarbon plus free water plus capillary water).
- Porosity vs permeability trends computed using FIB-SEM data and traditional "GRI" type data are similar.
- Data from plug samples, including SEM and FIB-SEM, can be upscaled by applying trends and correlations to the continuously sampled dual energy CT and SGR data.

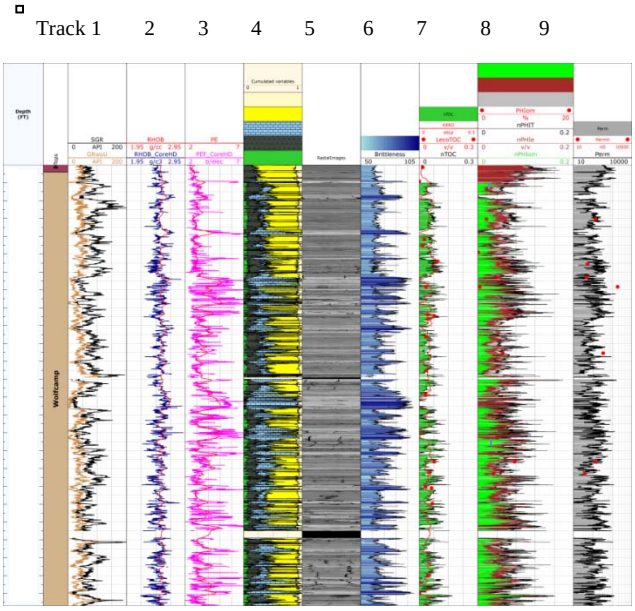

Figure 7: SGR, CT data, and computed curves. Track 1, spectral gamma; Track 2, RHOB, Track 3, PEF, Track 4, computed mineralogy; Track 5, radial images, Track 6, brittleness index; Track 7, TOC; Track 8, PAOM, PHIE, PHIT ; Track 9, permeability. Red curves are from well log data. Red data points are from plug samples. Cored interval is about 247 feet.

REFERENCES

1. Vinegar, Harold, X-ray CT and MR Imaging of Rocks, Journal of Petroleum Technology, March, 1986.
2. J.G.C. Coenen, J.G. Maas, Material classification by dual-energy computerized X-ray tomography, Proc. Int. Symp. on Computerized Tomography for Industrial Applications, 8–10 June 1994, Berlin, DGZfp, pp 120-127
3. Rickman, Rick, Mike Mullen, Erik Petre, Bill Geiser, Donald Kunert; A practical use of shale petrophysics for stimulation design optimization: all shale plays are not clones of the Barnett shale, presented at the SPE Annual Technical Conference and Exhibition, Denver, CO, 2008, SPE 115258.
4. Tolke, J., Baldwin, C., Mu, Y., Derzhi, N., Fang, Q., Grader, A., et al.: “Computer Simulations of Fluid Flow in Sediment: From Images to Permeability,” The Leading Edge, Vol. 29, No. 1, January 2010, pp. 68-74.
5. Chitale, Vivek D., 2010; Simplified and More Accurate Clay Typing Enhances the Value Added by Petrophysical Evaluation of Shale and Tight Gas Sand Plays, Search and Discovery Article #40487 (posted 2010), adapted from oral presentation at AAPG Convention, Denver, Colorado, June 7-10, 2009
6. Walls, J.D. and Sinclair, S.W.: “Eagle Ford Shale Reservoir Properties from Digital Rock Physics,” First Break, Vol. 29, No. 6, June 2011, pp. 97-101
7. Driskill, Brian, Joel Walls, Steven W. Sinclair, Juliana DeVito, “Applications of SEM Imaging to Reservoir Characterization in the Eagle Ford Shale, South Texas, USA”, from Electron Microscopy of Shale Hydrocarbon Reservoirs, Co-editors: Wayne Camp, Elizabeth Diaz, Barry Wawak, AAPG Memoir 102, April, 2013